J|A|C|S
ARTICLES
Published on Web 07/19/2002

Hydroxy Peroxy Nitrites and Nitrates from OH Initiated Reactions of Isoprene

Dan Zhang,[†] Renyi Zhang,*[,†] Jiho Park,[‡] and Simon W. North*[,‡]

Contribution from the Department of Atmospheric Sciences, Texas A&M University, College Station, Texas 77843, and Department of Chemistry, Texas A&M University, P.O. Box 30012, College Station, Texas 77842

Received January 3, 2002

Abstract: The reaction of hydroxy peroxy radicals (RO_2) with NO represents one of the most crucial tropospheric processes, leading to terrestrial ozone formation or NO_x removal and chain termination. We investigate the formation of hydroxy peroxy nitrites (ROONO) and nitrates ($RONO_2$) from the OH−isoprene reactions using DFT and ab initio theories and variational RRKM/master equation (vRRKM/ME) formalism. The binding energies of ROONO from NO addition to RO_2 are determined to be in the range of 20−22 kcal mol^{-1}, and the bond dissociation energies of ROONO to form an alkoxy radical (RO) and NO_2 range from 6 to 9 kcal mol^{-1}. Isomerization of ROONO to $RONO_2$ is exothermic by 22−28 kcal mol^{-1}. The entrance and exit channels of the RO_2−NO reaction are found to be barrierless, and the rate constants to form ROONO are calculated to be 3×10^{-12} to 2×10^{-11} cm^3 $molecule^{-1}$ s^{-1} using the canonical variational transition state theory. The vRRKM/ME analysis reveals negligible stabilization of excited ROONO and provides an assessment of ROONO isomerization to $RONO_2$.

Introduction

Because of its high chemical reactivity and role in the generation of peroxy radicals,[1−3] isoprene plays an important role in tropospheric chemistry.[4] The atmospheric oxidation of isoprene proceeds predominantly through OH radical addition to the isoprene double bonds, followed by reaction with O_2 to form the hydroxyperoxy radicals (Scheme 1).[2,5] In the presence of nitric oxide, the resulting hydroxyperoxy radical (RO_2) reacts with NO via the following two reaction pathways

$$C_5H_8OHO_2\bullet + NO \rightarrow C_5H_8OHO_2NO\bullet \quad (1)$$

$$C_5H_8OHO_2NO\bullet \rightarrow C_5H_8OHO\bullet + NO_2 \quad (2a)$$

$$\rightarrow C_5H_8OHONO_2 \quad (2b)$$

Reaction 2a is directly responsible for ozone formation, whereas reaction 2b results in NO_x removal and chain termination. It has been suggested that 50−100% of ozone production in some regional areas of the U.S. is because of reaction 2a (refs 1, 6, and 7), and as much as 7% of NO produced from fossil fuel combustion in North America in the summer is lost as nitrates formed because of reaction 2b (ref 7). In addition, the isoprene nitrates are responsible for about 4% of nitrogen oxides transported from North America.[8] Hence, the isoprene RO_2−NO reaction represents one of the most central tropospheric chemical problems of substantial impact.

Scheme 1

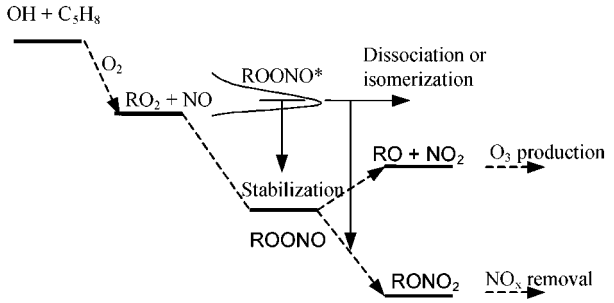

The entrance channel of the RO_2−NO reaction 1 is exoergic (Scheme 1), leading to a vibrationally excited hydroxyperoxy nitrite (ROONO*), which subsequently reacts via unimolecular reactions or collisional stabilization. The excited ROONO* undergoes two possible prompt unimolecular reactions, isomerization to the isoprene nitrate ($RONO_2$) or decomposition to a hydroxyalkoxy radical (RO) and NO_2. Similarly, there are two plausible reaction pathways for the thermalized ROONO,

* To whom correspondence should be addressed. E-mail: zhang@ariel.met.tamu.edu (R.Z.); north@chem.tamu.edu (S.W.N.).
[†] Department of Atmospheric Sciences, Texas A&M University.
[‡] Department of Chemistry, Texas A&M University.

(1) (a) Trainer, M.; et al. *Nature* **1987**, *329*, 705. (b) Rasmussen, R. A.; Khalil, M. A. *J. Geophys. Res.* **1988**, *93*, 1417.
(2) Atkinson, R. *J. Phys. Chem. Ref. Data* **1997**, *26*, 251.
(3) Seinfeld, J. H.; Pandis, S. N. *Atmospheric Chemistry and Physics: From Air Pollution to Climate Change*; John Wiley & Sons: New York, 1997.
(4) (a) Chameides, W. L.; Lindsay, R. W.; Richardson, J.; Kiang, C. S. *Science* **1988**, *241*, 1473. (b) Jacob, D. J.; Wofsy, S. C. *J. Geophys. Res.* **1988**, *93*, 1477. (c) Zhang, R.; Suh, I.; Clinkenbeard, A. D.; Lei, W.; North, S. W. *J. Geophys. Res.* **2000**, *105*, 24627.
(5) Lei, W.; Zhang, R.; McGivern, W. S.; Derecskei-Kovacs, A.; North, S. W. *J. Phys. Chem.* **2001**, *105*, 471.
(6) Wiedinmyer, C.; Friedfeld, S.; Baugh, W.; Greenberg, J.; Geunther, A.; Fraser, M.; Allen, D. *Atmos. Environ.* **2001**, *35*, 1001.
(7) Chen, X. H.; Hulbert, D.; Shepson, P. B. *J. Geophys. Res.* **1998**, *103*, 25563.
(8) Horowitz, L. W.; Liang, J.; Gardner, G. M.; Jacob, D. J. *J. Geophys. Res.* **1998**, *103*, 13451.

10.1021/ja0255195 CCC: $22.00

decomposition to RO and NO_2 or isomerization to form $RONO_2$. The complexity of the RO_2-NO reaction further arises from the presence of possible structural isomers; there are four β- and two δ-hydroxyperoxy radicals from the OH-initiated reactions of isoprene.[5]

Despite the fundamental importance of isoprene oxidation, the nature of the isoprene RO_2-NO reaction remains highly uncertain. There are several reasons to believe that the isoprene chemistry will be distinct from simpler hydrocarbons. Unlike the analogous species associated with the oxidation of smaller hydrocarbons, there are multiple isomers, and hence the kinetics will exhibit multiexponential behavior.[9] Also, because the activated nitrites are significantly larger, they undergo slower unimolecular reaction, and the kinetics should experience greater pressure dependence. Furthermore, there likely exists hydrogen bonding in the isoprene species, which plays an important role in determining their structural characteristics, stability, and chemistry. Experimental studies have identified nonnegligible nitrate yield from the OH-initiated reactions of isoprene,[10,11] in contrast to the observed absence of nitrate formation from oxidation of smaller alkenes.[2,12]

In this paper, we report a theoretical study of the ROONO and $RONO_2$ species derived from the OH−isoprene reactions to elucidate the chemistry of the RO_2-NO reaction. Density functional theory (DFT) and ab initio methods were employed to investigate the structures and energetics of those species. Canonical variational transition state theory (CVTST) was employed to calculate the rate constants for the RO_2-NO reaction. In addition, variational RRKM/master equation (vRRKM/ME) calculations were carried out to assess stabilization of the excited hydroxy peroxy nitrite and to evaluate nitrate formation of the OH−isoprene reactions.

Theoretical Method

The quantum chemical computations were performed on an SGI Origin 3800 supercomputer using the Gaussian 98 software package.[13] Geometry optimization for all species was executed using Becke's three parameter hybrid method employing the Lee−Yang−Parr correlation function (B3LYP)[14] in conjunction with the split valence polarized basis set 6-31G(d,p). The DFT geometries were then employed in single-point energy calculations using frozen-core second-order Møller−Plesset perturbation theory (MP2) and coupled-cluster theory with single and double excitations including perturbative corrections for the triple excitations (CCSD(T)) with various basis sets. Harmonic vibrational frequency calculations were made using B3LYP/6-31G(d,p). Additional geometry optimization using MP2/6-31G(d,p) was also performed to verify the DFT structures.

We have recently evaluated the level of ab initio theory that applies to complex organic intermediates, on the basis of computational efficiency and accuracy.[15] We found that better convergence behavior and considerably higher computational efficiency were achieved using the density function theory as the method of geometry and frequency calculations. In addition, our studies for the analogous reactions of OH, Cl, NO_3, or O_3 addition to isoprene indicated that the calculated energetics were very sensitive to effects of basis set and electron correlation.[5,15−18] To obtain accurate energetics, a basis set correction factor (CF) method was applied to the CCSD(T) calculated energies of all stationary points on the basis of an approach developed to investigate the OH−isoprene reaction.[15] The procedure involved determination of a correction factor associated with basis set effects at the MP2 level and subsequent correction to the energy calculated at a higher level of electron correlation with a moderate size basis set. The basis set effect on the energies was evaluated at the MP2 level. A correction factor (CF) was determined from the energy difference between the MP2/6-31G(d) and MP2/6-311++G(d,p) levels. The values of calculated energies at the CCSD(T)/6-31G(d) level were then corrected by the MP2 level correction factors, corresponding to the CCSD(T)/6-31G(d) + CF method. This method, which is effective to the CCSD(T)/6-311++G(d,p) level of theory, has been evaluated extensively for several isoprene addition reactions.[15−18]

Results and Discussion

Structures and Energetics of ROONO and $RONO_2$. Considering the large amount of possible spatial orientations for the O−O−N−O group in the ROONO isomers as well as existence of a chiral carbon center, it is of considerable challenge to locate the global minima of the equilibrium structures. Geometry optimizations of the ROONO isomers were initially performed using the geometries of the corresponding peroxy radicals,[5] by adding NO to the terminal O atom. The main carbon chain was kept unchanged from the corresponding peroxy radical, but the relative position of the O−O−N−O group was varied with respect to the carbon chain. Three important parameters were considered, that is, the torsion angles of C−C−O−O, C−O−O−N, and O−O−N−O, along with the relative orientations of the O−O−N−O group to the OH and methyl groups. Figure 1 depicts the optimized geometries of the lowest-energy conformations of the ROONO isomers. The evaluation of the vibrational frequencies confirmed that all geometries reported represent minima on the potential energy surfaces.

Comparison of the equilibrium geometries of ROONO with those of corresponding RO_2 and RO obtained previously[5,17] reveals some intriguing features. The torsion angles of O(H)−C1−C2−O for RO_2, ROONO, and RO are not very different, indicating that addition of NO or removal of an O atom has little effect on the structure of the main carbon chain and the attached O atom. However, the two torsion angles of C3C2OO and C1C2OO for RO_2 and ROONO are significantly different, implying that addition of the NO group changes the O−O bonding. Another interesting feature is the change of the corresponding C−C and C−O bond lengths for RO_2, ROONO, and RO. Addition of NO to the peroxy radicals leads to a shortening of the C−O bond from 1.47 to 1.49 Å for RO_2 to 1.448−1.461 Å for ROONO, but a lengthening of the O−O bond from 1.32 Å for RO_2 to 1.434−1.456 Å for ROONO. This results from the redistribution of the electron cloud of the two

(9) Zhang, D.; Zhang, R.; Church, C.; North, S. *Chem. Phys. Lett.* **2001**, *343*, 49.
(10) O'Brien, J. M.; Czuba, E.; Hastie, D. R.; Francisco, J. S.; Shepson, P. B. *J. Phys. Chem. A* **1998**, *102*, 8903.
(11) Tuazon, E. C.; Atkinson, R. *Int. J. Chem. Kinet.* **1990**, *22*, 1221.
(12) Orlando, J. J.; Tyndall, G. S.; Bilde, M.; Ferronato, C.; Wallington, T. J.; Vereechen, L.; Peeters, J. *J. Phys. Chem.* **1998**, *102*, 8816.
(13) Frisch, M. J.; Trucks, G. W.; Schlegel, H. B.; Gill, P. M. W.; Johnson, B. G.; Robb, M. A.; Cheeseman, J. R.; Keith, T.; Petersson, G. A.; Montgomery, J. A.; Raghavachari, K.; Al-Laham, M. A.; Zakrzewski, V. G.; Ortiz, J. V.; Foresman, J. B.; Cioslowski, J.; Stefanov, B. B.; Nanayakkara, A.; Challacombe, M.; Peng, C. Y.; Ayala, P. Y.; Chen, W.; Wong, M. W.; Andres, J. L.; Replogle, E. S.; Gomperts, R.; Martin, R. L.; Fox, D. J.; Binkley, J. S.; Defrees, D. J.; Baker, J.; Stewart, J. P.; Head-Gordon, M.; Gonzalez, C.; Pople, J. A. *Gaussian 98*, revision D.3; Gaussian, Inc.: Pittsburgh, PA, 1998.
(14) (a) Becke, A. D. *J. Chem. Phys.* **1992**, *96*, 2155. (b) Becke, A. D. *J. Chem. Phys.* **1993**, *98*, 5648. (c) Lee, C.; Yang, W.; Parr, R. G. *Phys. Rev. B* **1988**, *37*, 785.
(15) Lei, W.; Derecskei-Kovacs, A.; Zhang, R. *J. Chem. Phys.* **2000**, *113*, 5354.
(16) Lei, W.; Zhang, R. *J. Chem. Phys.* **2000**, *113*, 153. (b) Suh, I.; Lei, W.; Zhang, R. *J. Phys. Chem.* **2001**, *105*, 6471.
(17) Lei, W.; Zhang, R. *J. Phys. Chem.* **2001**, *105*, 3808.
(18) Zhang, D.; Zhang, R. *J. Am. Chem. Soc.* **2002**, *124*, 2692.

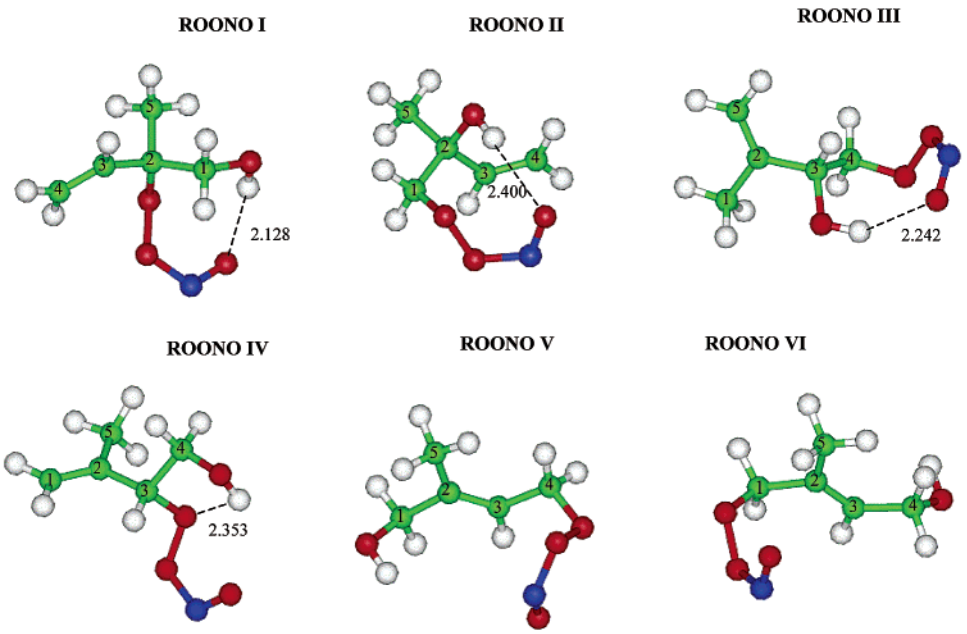

Figure 1. Structures of hydroxy peroxy nitrites (ROONO) at the B3LYP/6-31G(d,p) level of theory.

Table 1. Binding Energies (D_0) for $RO_2 + NO \rightarrow$ ROONO, Bond Dissociation Energies (D_e) for ROONO $\rightarrow$ RO + NO_2, Reaction Energies (ΔE) for ROONO $\rightarrow$ $RONO_2$, and Relative Energies (*RE*) of ROONO[a]

	D_0			D_e			ΔE			*RE*
	B3LYP/ 6-31G(d,p)	CCSD(T)/ 6-31G(d)	CCSD(T)/6- 31G(d) + CF	B3LYP/ 6-31G(d,p)	CCSD(T)/ 6-31G(d)	CCSD(T)/6- 31G(d) + CF	B3LYP/ 6-31G(d,p)	CCSD(T)/ 6-31G(d)	CCSD(T)/6- 31G(d) + CF	CCSD(T)/6- 31G(d) + CF
I	20.4	20.7	20.2	6.4	13.0	7.5	−22.2	−18.6	−22.7	1.2
II	21.5	21.6	21.2	7.0	12.8	8.0	−26.7	−22.3	−26.0	0
III	21.9	22.0	21.2	6.9	13.2	7.9	−25.8	−21.7	−25.4	1.6
IV	21.6	21.7	20.6	6.4	13.9	8.7	−26.7	−23.0	−26.8	1.3
V	21.8	21.3	20.9	7.9	13.7	9.4	−27.1	−22.9	−25.3	4.8
VI	22.0	21.7	21.2	8.1	13.7	9.7	−26.2	−22.3	−25.0	5.1

[a]All energies have included in them the zero-point correction.

O atoms in the peroxy radical because of formation of the new O−N bond. The lowest-energy conformers of ROONO **V** and **VI** possess trans structures, similar to the corresponding isomers of RO_2 but different from those of RO which possess cis structures. The trans configurations of ROONO **V** and **VI** are more stable than the cis configurations by 0.3 and 1.7 kcal mol^{-1}, respectively.

It is evident from Figure 1 that there exists intramolecular hydrogen bonding in the β-ROONO isomers **I**−**VI**. The hydrogen bond involves the terminal O atom from the O−O−N−O group and the H atom from the hydroxy group. The length of the hydrogen bond ranges from 2.1 to 2.4 Å, slightly longer than a typical hydrogen bond length. The relatively weak hydrogen bonding is explained by the fact that it involves a five- to eight-member ring. It is also clear in Figure 1 that no such intramolecular hydrogen bond forms for the δ-ROONO isomers **V** and **VI**, because of the relatively long distance between the nitrite and hydroxy groups.

The energetics of the ROONO species was calculated with various ab initio levels of theory. Table 1 lists binding energies calculated for the NO−RO_2 reaction to form ROONO. Generally, the MP2 method systematically predicts higher binding energies than the B3LYP and CCSD(T) methods. The correction factor (CF) was derived from the difference of the MP2 calculated energies as described previously, with the values ranging from 0.3 to 0.9 kcal mol^{-1}. The binding energies predicted with B3LPY/6-31G(d,p) and CCSD(T)/6-31G(d) + CF are quite similar, with a largest difference of 1.0 kcal mol^{-1} for ROONO **III**. It is also interesting to compare the relative stability between the ROONO isomers. The β-ROONO isomers **I**−**IV** are 4−5 kcal mol^{-1} more stable than the two δ-ROONO isomers **V** and **VI**, suggesting a stabilization effect because of hydrogen bonding in the β-ROONO isomers. Table 1 also summarizes the bond dissociation energies calculated for the reaction ROONO $\rightarrow$ RO + RO_2. The inclusion of the correction factor improves the agreement between the B3LYP and CCSD(T) methods, and the difference between B3LYP/6-31G(d,p) and CCSD(T)/6-31G(d) + CF ranges from 1.1 to 2.3 kcal mol^{-1}.

Figure 2 illustrates the equilibrium structures of the $RONO_2$ isomers. As is the case with ROONO, there appears to exist hydrogen bonding for the β-ROONO isomers **I**−**IV**, with the length of 2.332−2.437 Å. These bond distances are slightly longer than those of the corresponding ROONO isomers, except for isomer **II**. Also, there is a noticeable absence of such a hydrogen bond in the two δ-$RONO_2$ isomers **V** and **VI**. The reaction energies for isomerization of ROONO to $RONO_2$ are also given in Table 1. The B3LYP/6-31G(d,p) results are generally in agreement with the CCSD(T)/6-31G(d) + CF values

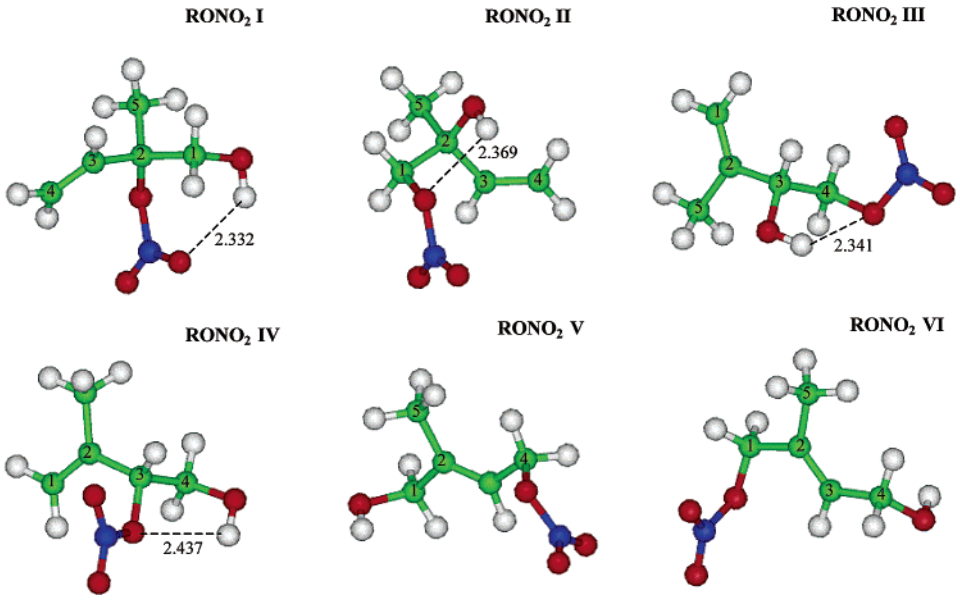

Figure 2. Structures of hydroxy nitrates ($RONO_2$) at the B3LYP/6-31G(d,p) level of theory.

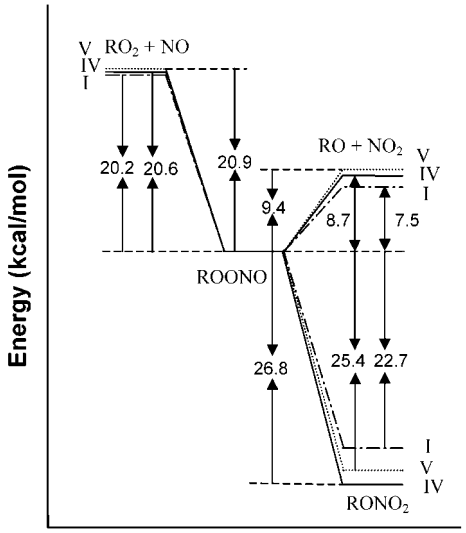

Figure 3. Potential energy surface (PES) of the RO_2-NO reaction obtained by using CCSD(T)/6-31G(d) + CF//B3LYP/6-31G(d,p).

for all isomers, with the largest difference of 1.8 kcal mol^{-1} for isomer **V**.

A potential energy surface of the RO_2-NO reaction sequence is shown in Figure 3 for isomers **I**, **IV**, and **V**. The combination of RO_2 and NO is exothermic by about 20 kcal mol^{-1}. Rearrangement of ROONO to $RONO_2$ is exothermic by 23−27 kcal mol^{-1}. The O−O bond dissociation energies of ROONO range from 7 to 10 kcal mol^{-1}, smaller than the literature estimates for HO−ONO and other non-nitrogen C_1-C_4 RO−OR′ species.[19] This occurs because of the fact that large substitutes and nitrogen-containing groups reduce the binding energy.

Entrance Channel of the RO_2-NO Reaction. To evaluate the nature of the entrance channel of the RO_2-NO reaction, we have examined the potential along the reaction coordinate, specifically whether there is a well-defined transition state or the addition proceeds without a barrier via a loose transition state. We performed constrained geometry optimization at the B3LYP/6-31G(d) level of theory for fixed O−N bond lengths. We find no energy exceeding the bond dissociation energy along the reaction coordinate.

The rate constant of the reaction of RO_2 with NO was calculated by using the CVTST method. Briefly, the association rate is related to the dissociation rate by[5,20]

$$\frac{k_{rec}}{k_{uni}} = \frac{Q_{AB}}{Q_A Q_B} \exp\left(\frac{D_0}{kT}\right) \tag{3}$$

where Q_{AB} is the partition function of ROONO, Q_A and Q_B are the partition functions of the respective RO_2 and NO, and D_0 is the zero-point-corrected binding energy of ROONO. The unimolecular dissociation of each isomer was calculated according to the following expression[5,20]

$$k_{uni} = \frac{kT}{h} \frac{Q^{\ddagger}_{AB}}{Q_{AB}} \exp\left(-\frac{\Delta E'}{kT}\right) \tag{4}$$

where $Q^{\ddagger}_{AB}$ is the partition function of the transition state with the vibrational frequency corresponding to the reaction coordinate removed, and $\Delta E'$ is the zero-point-corrected transition state energy relative to the ROONO minimum. Because NO addition to RO_2 proceeds without an activation barrier, the location of the transition state was determined variationally by minimizing the reaction rate.

The partition functions required for eqs 3 and 4 were evaluated by treating the rotational and translational motion classically and treating vibrational modes quantum mechanically. Unscaled vibrational frequencies and moments of inertia were taken from the B3LYP/6-31G(d,p) calculations, and the reaction energies were taken from the zero-point-corrected CCSD(T)/6-31G(d) + CF. The dependence of the transitional mode frequencies with O−N distance was modeled using[5,20]

(19) Bach, R. D.; Ayala, P. Y.; Schlegel, H. B. J. *Am. Chem. Soc.* **1996**, *118*, 12758.

(20) (a) Lei, W.; Zhang, R.; McGiven, W. S.; Derecskei-Kovacs, A.; North, S. W. *Chem. Phys. Lett.* **2000**, *326*, 109. (b) McGiven, S.; Suh, I.; Clinkenbeard, A. D.; Zhang, R.; North, S. W. *J. Phys. Chem.* **2000**, *104*, 6609.

$$\nu(r) = \nu_0 \exp[-a(r - r_e)] + B \quad (5)$$

where ν_0 is the vibrational frequency in the reactant molecule, r_e is the equilibrium bond distance, B is the sum of the rotational constants, and a is a constant estimated on the basis of ab initio calculations of the vibrational frequencies along the reaction coordinates. The potential energy surface along the reaction coordinate was modeled by a Morse function including the centrifugal barrier

$$V(r) = D_0[1 - \exp(-\beta r)]^2 + B_{ext}(r)J(J+1) \quad (6)$$

where D_0 is the binding energy, $B_{ext}(r)$ is the external rotational constant determined using the symmetric top moment of inertia, and J is the average rotational quantum number of a Boltzmann distribution calculated using the external rotational constant of the molecule at the equilibrium configuration.

The CVTST calculated high-pressure limit rate constants for the formation of the ROONO isomers at 300 K are presented in Table 2. Also given in this table for comparison are the relative branching ratios for ROONO, with the isomers **I**, **IV**, and **V** constituting the majority of the total nitrite population.[5] The calculated rate constants range from 3.3×10^{-12} to 1.3×10^{-11} cm^3 molecule^{-1} s^{-1}. The rates to form isomers **IV** and **V** are comparable, while the rates to form the other isomers are much slower. Hence, the kinetics of the isoprene RO_2-NO reaction shows a strong multiexponential behavior. The sensitivity of the rate constants to the binding energies was examined by recalculating the rate constants for the six isomers using binding energies which differed by ± 2 kcal mol^{-1} from the ab initio energies. In both cases, the individual rates changed by less than 50%. We estimated that the uncertainty in the calculated rate constant is within a factor of 2.

Two experimental studies have indirectly inferred the effective rate constant for the isoprene RO_2-NO reaction, on the basis of fitting the time-dependent OH signal in the presence of OH, isoprene, O_2, and NO.[21] The previously reported experimental values are 9×10^{-12} and $(2.5 \pm 0.5) \times 10^{-11}$ cm^3 molecule^{-1} s^{-1}. Our theoretical calculations of the isoprene RO_2-NO rate constant are consistent with the previous experimental results.

The Fate of Excited ROONO*. There are three possible reaction pathways for the excited ROONO*: collisional stabilization, prompt isomerization to $RONO_2$, or prompt dissociation to RO and NO_2. Although equilibrium favors reaction 2a over 2b on the basis of the calculated energetics, the relative importance of each pathway is determined by complex kinetics.

We have performed calculations to assess the fate of the excited hydroxyperoxy nitrites derived from isoprene oxidation using the steady-state master equation (ME) formalism[18,22] in conjunction with the variational-RRKM method. We adopted a Morse potential that includes the centrifugal barrier to variationally locate the transition states for NO addition to the hydroxyperoxy radical as a function of energy. As above-noted, our treatment of the entrance channel of the $NO-RO_2$ reaction for a barrierless pathway is consistent with experimentally observed weak temperature dependence for this type of reactions,[2] and our vRRKM calculations are qualitatively in agreement with an efficient rate constant on the order of 10^{-11} cm^3 molecule^{-1} s^{-1}. Similarly, we found that dissociation of ROONO to RO and NO_2 also proceeds through a barrierless process, because the calculated energy relative to the equilibrium peroxynitrite increased monotonically when the O−O bond length was successively increased. Nitrite dissociation was also treated using vRRKM theory. Exact state counts for the entrance and exit channels and hydroperoxynitrite vibration density of states were evaluated by using the Beyer−Swinehart algorithm.[23] The vibrational frequencies were modified along the reaction coordinate according to an exponential switching model.[24,25] The vRRKM/ME calculations employed an exponential model for collision energy transfer using an average energy of 250 cm^{-1}. A Lennard-Jones collision frequency of $Z_{LJ} = 1.4 \times 10^{10}$ s^{-1} at 298 K and 760 Torr was estimated using values of $\sigma = 6.57$ Å and $\epsilon = 567$ K. All vibrations were treated as harmonic. We found that explicit treatment of the internal rotors as hindered rotors did not significantly alter the results. Calculations were performed at fixed total angular momentum and were subsequently Boltzmann averaged.

Table 2. CVTST Calculated High-Pressure Limit Rate Constants of $RO_2 + NO \rightarrow ROONO$ at 300 K[a]

species	rate constant (cm^3 molecule^{-1} s^{-1})	branching ratio
I	3.2×10^{-12}	0.34
II	6.7×10^{-12}	0.02
III	9.6×10^{-12}	0.05
IV	1.3×10^{-11}	0.29
V	1.3×10^{-11}	0.22
VI	7.0×10^{-12}	0.08

[a] Also shown in the table are isomeric branching ratios determined previously.[5]

The vRRKM dissociation rates for ROONO isomer **1** as a function of energy relative to the nitrite well are shown in Figure 4. Also plotted in the figure is the initial nitrite energy distribution. At all energies above the entrance channel (20.2 kcal mol^{-1}), the dissociation rates are larger than the collision rate. We conclude that there is insignificant formation of thermalized nitrite under ambient conditions. On average, only 1−4 kcal mol^{-1} of nitrite internal energy is lost to collisions. Dissociation of ROONO* leads to activated RO*, which also reacts via unimolecular reactions or is collisional stabilized. For both thermalized and activated β-RO radicals, their dominant fate is decomposition, leading to the formation of various oxygenated organic compounds.[17]

It was previously suggested that rearrangement of the peroxynitrite to nitrate proceeds via a three-centered transition state which for HOONO corresponds to an activation energy of ~60 kcal mol^{-1}.[26] However, the three-centered transition state is likely hindered by the substitute of a carbon chain to the hydrogen atom,[10] and the rearrangement of ROONO to $RONO_2$ may go through a partial O−O bond fission followed by RO

(21) (a) Steven, P.; L'Esperance, D.; Chuong, B.; Martin, G. *Int. J. Chem. Kinet.* **1999**, *31*, 637. (b) Reitz, J. E.; McGiven, W. S.; Church, M. C.; Wilson, M. D.; North, S. W. *Int. J. Chem. Kinet.* **2002**, *33*, 637.
(22) Gilbert, R. G.; Smith, S. C. *Theory of Unimolecular and Recombination Reactions*; Blackwell Scientific: Oxford, U.K., 1990.
(23) Stein, S. E.; Rabinovitch, B. S. *J. Chem. Phys.* **1973**, *58*, 2438.
(24) Holbrook, K.; Pilling, M.; Robertson, S. *Unimolecular Reactions*; John Wiley & amp, Sons: Chichester, 1996.
(25) We have used values of $a = 1.9$ Å^{-1} and $a = 1.2$ Å^{-1} for the entrance and exit channels of the RO_2-NO reaction, respectively, based on ab initio calculations of the vibrational frequencies along the reaction coordinates.
(26) (a) Houk, K. N.; Condroski, K. R.; Pryor, W. A. *J. Am. Chem. Soc.* **1996**, *118*, 13002. (b) Cameron, D. R.; Borrejo, A. M. P.; Bennett, B. M.; Thatcher, G. R. J. *Can. J. Chem.* **1995**, *73*, 1627. (c) Jursic, B. S.; Klasine, L.; Pecur, S.; Pryor, W. A. *Nitric Oxide* **1997**, *1*, 494.

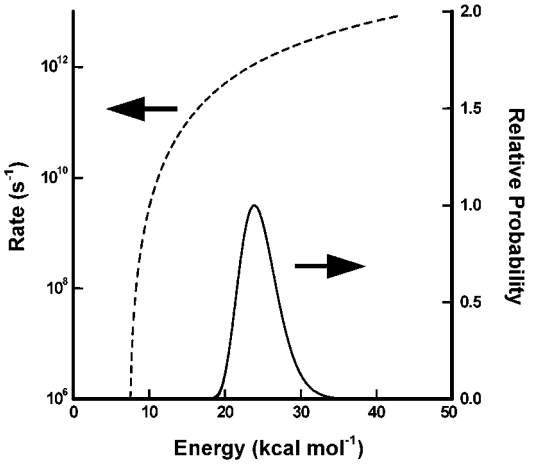

Figure 4. Hydroxy peroxy nitrite (ROONO) vRRKM dissociation rates for isomer **1** as a function of microcanonical energy (dashed curve). For comparison, the collision rate is 1.4×10^{10} s^{-1} at 760 Torr and 298 K. Also shown is the initial energy distribution of the nitrite radicals (solid curve). All energies are relative to the bottom of the nitrite well.

Table 3. Barrier Heights (kcal mol^{-1}) for ROONO → $RONO_2$ Isomerization Estimated on the Basis of vRRKM/ME Calculations[a]

	I	II	III	IV	V	VI
isomerization (A)	7.0	7.4	7.1	7.7	8.2	8.1
isomerization (B)	11.1	11.6	11.6	12.2	12.8	13.2
dissociation	7.5	8.0	7.9	8.7	9.4	9.7

[a]Also shown in the table for comparison are bond dissociation energies of ROONO.

and NO_2 recombination at elongated O−O bond lengths. We were unable to locate the transition state for nitrite−nitrate isomerization. It is possible, though, to provide an estimate of the upper and lower limits to the barrier height by treating the vibrational frequencies of the transition state in two limiting approximations. Several experimental studies have reported the nitrate yield from the OH-initiated oxidation of isoprene, ranging from 4 to 12%.[10,11] We have chosen to adjust the barrier heights to match the 0.05 fraction of nitrate formation, suggested by the work of Shepson and co-workers,[10] employing the vRRKM/ME formalism. The results of this treatment are shown in Table 3. In the first case (model A), the frequencies of the nitrite are used to mimic a tight transition state. Because the nitrite yield is much lower than the dissociation yields, the resulting barrier heights are lower than the corresponding dissociation energies. The second approximation (model B) assumes that the isomerization transition state is loose and can be modeled by treatment identical to that of the dissociation, adjusting the asymptotic energy to give 0.05 fractional yield. This results in a higher barrier in energy relative to dissociation. It is unlikely that the transition state associated with isomerization will be looser than the barrierless dissociation, so both treatments serve to bracket the energy of the real transition state. The vRRKM/ME analysis predicts that the activation barrier of ROONO isomerization to $RONO_2$ is between 0.4 and 1.1 kcal mol^{-1} below and 3.3−3.7 kcal mol^{-1} above the dissociation energy of ROONO. The isomerization barrier heights derived from either approximation are significantly lower than the barrier height for the three-center transition state in HOONO.[26]

Conclusions

In this paper, we have presented a theoretical investigation of the isoprene RO_2−NO reaction, one of the most crucial tropospheric chemical processes. DFT and ab initio methods have been employed to obtain the structures and energetics of the isoprene hydroxy peroxy nitrites and nitrates, and CVTST and vRRKM/ME calculations have been performed to investigate the reaction kinetics and mechanism. The results provide several novel aspects for refinement and quantification of the photochemical oxidation of isoprene in the atmosphere.

(1) The structures and energetics of hydroxy peroxy nitrites and nitrates arising from OH-initiated reactions of isoprene have been first obtained. The binding energies of ROONO range from 20 to 22 kcal mol^{-1}. The bond dissociation energies of ROONO to RO and NO_2 are in the range of 6−9 kcal mol^{-1}. Isomerization of ROONO to $RONO_2$ is exothermic by 22−28 kcal mol^{-1}. The β-ROONO isomers exhibit hydrogen bonding and are more stable than the δ-ROONO isomers.

(2) The entrance and exit channels of the RO_2−NO reaction are found to be barrierless. The rate constants of the RO_2−NO reaction are calculated in the range from 3.3×10^{-12} to 1.3×10^{-11} cm^3 molecule^{-1} s^{-1}, showing a strong multiexponential kinetic behavior.

(3) The vRRKM/ME calculations reveal insignificant stabilization of excited ROONO* and provide estimates of the barrier heights for ROONO isomerization to $RONO_2$.

Acknowledgment. This work was supported by the Robert A. Welch Foundation (A-1417) and Texas Advanced Research Program (Chemistry). Additional support for this work was provided by the Texas A&M University Supercomputing Facilities. We thank Dr. Lisa Thomson for helpful discussions and acknowledge the use of the Laboratory for Molecular Simulations at the Texas A&M University. Three referees provided helpful comments for improving this manuscript.

Supporting Information Available: Absolute energies, zero-point energies, vibrational frequencies, and the structural parameters for all of the species investigated in this study (PDF). This material is available free of charge via the Internet at http://pubs.acs.org.

JA0255195